Investigations on the durability of alkali-activated recycled glass

Rachida Idir, Martin Cyr, Alexandre Pavoine

Investigations on the durability of alkali-activated recycled glass

Rachida IDIR[a*], Martin CYR[b], Alexandre PAVOINE[a]

[a] Cerema, DIMA Project team, 120, rue de Paris - BP 216 - Sourdun - 77487 Provins CEDEX

[b] Université de Toulouse, UPS, INSA, Laboratoire Matériaux et Durabilité des Constructions, 135, avenue de Rangueil, F-31077 TOULOUSE Cedex 4, France

*Corresponding author: Rachida IDIR

Phone: (+33) 1 60 52 34 04

Email: rachida.idir@cerema.fr

Abstract

This work undertakes research on alkali-activated glass cullet (AAGC), with glass being recycled from various sources. Three types of glass are studied and compared: flat glass, hollow glass, and windshield glass. The study conducted yields the main formulation parameters affecting the behavior of AAGC, namely the concentration of activation solution KOH (1, 2, 3, 5, 7 and 10 mol/l) and the curing duration (1, 2, 4, 7 and 14 days) at 60°C. These parameters are evaluated in terms of both compressive strength and flexural strength. Different durability parameters are also examined in this work, i.e.: porosity accessible to water, capillary absorption, chloride ion diffusion, sulfate attack, acid attack, and the alkali-silica reaction. Results show that for all three recycled glass types, optimal synthesis occurs under the condition with 3 mol/l KOH and 7 days of curing at 60°C. Durability tests reveal that AAGC synthesized from these three recycled glasses exhibit an acceptable resistance to acid solution, sulfate attack and alkali-silica reaction despite their high permeability compared with ordinary Portland cement (OPC).

Keywords

Recycled glass, alkali-activated materials, diffusion of chloride ions, sulfate attack, acid attack, alkali-silica reaction, carbonation

1. Introduction

Alkali-activated materials such as geopolymers, as an alternative to Portland cement (Davidovits, 1991; Duxson *et al.*, 2007), have gained popularity over the last two decades. The term "geopolymer" is used herein to describe aluminosilicate inorganic polymers (Davidovits, 1991, 1993), which can be produced by synthesizing pozzolanic compounds or aluminosilicate materials with highly alkaline solutions. The possibility of varying the Si/Al molar ratio, hence the structure and physicochemical properties of the geopolymers, extends the scope of application of these materials. Most studies however have been limited to the use of certain fine minerals such as metakaolin (Zibouche *et al.*, 2009; Aly *et al.*, 2008), silica fume (Prud'homme *et al.*, 2010; Panias *et al.*, 2007; Komljenovic *et al.*, 2010), blast-furnace slag (Maragkos *et al.*, 2009; Mozgawa *et al.*, 2009; Mohammadinia *et al.*, 2016), fly ash (Palomo *et al.*, 1999; Kabir *et al.*, 2015,), natural pozzolana (Peng *et al.*, 2017), red mud (Ke *et al.*, 2015) or rice hull ash (Hajimohammadi *et al.*, 2017; Sturm *et al.*, 2016). In fact, all these materials are capable of supplying the reaction medium with silica and aluminum, both of which are necessary for the polymerization reaction. Cyr *et al.* (2012) demonstrated that soda-lime-silica glass, despite its low aluminum content, could be activated by an alkaline solution to form alkali-activated-like materials. Alkali-activated glass offers an

alternative solution for introducing recycled glass when typical recycling routes are not available. For instance, the use of recycled glass as aggregates in new concretes may lead to an alkali-silica reaction due to the high amorphous silica and alkali contents in the recycled glass (Stanton, 1940). In the case of alkali-activated glass, the high contents of these elements can be seen as an advantage during the synthesis of alkali-activated materials (Cyr *et al.*, 2012) because both components are involved in the alkali-activation reaction.

Three types of recycled glass have been studied in this work: recycled window glass, hollow glass, and windshield glass. While these glass types benefit from recycling, the routes available are indeed limited, thus prompting the exploration of new applications. Recycled window glass can be recovered from construction waste; however, this kind of glass is difficult to reuse in the glass industry since the waste it generally contains cannot satisfy the glass company's purity requirement. Recycled hollow glass accounts for a large share of collected glass and is typically recycled to produce new packaging containers. Nonetheless, a fraction of this glass cannot be easily recycled (e.g. small particles may not be reused since they are considered harmful to the furnace). Recycled windshield glass originates from vehicle waste, yet the recycling process focuses mainly on the reuse of metal components (e.g. 75% of a car).

The objective of this paper is to explore the possibilities of reusing these three recycled glass types as construction materials. The alkali-activation of this recycled glass is studied by verifying different pairs of test conditions, namely KOH concentrations and curing times. The durability of AAGC mortars is also evaluated herein: transfer properties (porosity, capillary coefficient and diffusion), internal attacks (alkali-silica reaction), external attacks (sulfate attacks and acid attack), and structural reinforcement (carbonation).

2. Materials and methods

2.1 Materials

Three types of glass have been used in this work: flat glass (G_F), hollow glass (G_H), and windshield glass (G_W) (see Fig 1). Table 1 lists their physical and chemical characterizations. All glass specimens were ground to a powder with similar specific surface areas (as determined by the *Blaine method: NF EN 196-6*) of around 4,000 cm^2/g. This value was set according to Cyr *et al.* (2012) since the alkali-activated mortars prepared using this specific surface area of glass have displayed good mechanical performance. All these specimens were primarily composed of a high quantity of silica (70~72%) with ~14% alkali (Na_2O), a large quantity of oxide calcium (8~12%) and a slight amount of oxide aluminum (1~2%). A difference was noted for G_F, which contained less aluminum and calcium (but more MgO) than either G_H or G_W.

The 0-2 mm sand used in the mortars was quartz according to Standard EN 196-1 (AFNOR, 2006a). The alkaline activator during the investigation was potassium hydroxide, prepared at concentrations of 1, 2, 3, 5, 7 and 10 mol/l by dissolving KOH pellets in distilled water. KOH was chosen rather than NaOH because previous work showed that it was the most effective activator (Cyr *et al.* 2012). It is to highlight that the pH of the solutions used is very high. Safety precautions are taken when such solutions are handled.

[Insert Fig. 1 here]

Fig 1: Glass powders obtained after grinding

Table 1: Physical and chemical characterizations of the studied glass types

[Insert Table 1 here]

2.2 Methods

The mortars cast were composed of three parts sand and one part glass (by mass). The alkaline solution-to-glass ratio equaled 0.5 (by mass). The mortars were mixed according to European Standard EN 196-1. Each layer of mortar was vibrated for 30 s in order to release air bubbles. The molds were sealed in plastic bags to minimize moisture loss and then stored directly at 60°C. The specimens were demolded 1 day after casting, then sealed in plastic bags and cured under different study conditions, i.e.:

- At 60°C for 1, 2, 4, 7 and 14 days respectively, then cooled to room temperature for compressive strength tests.
- At 60°C for 7 days, and then cooled at room temperature (24 h) for the durability tests.

2.3 Experimental program

Figure 2 summarizes the experimental program carried out as part of the study, with each test being conducted on three replicate samples.

[Insert Fig. 2 here]

Fig. 2: Summary of the experimental program part of the study

- The compressive strength and flexural strength tests were performed with 4x4x16 cm prism specimens according to European Standard NF EN 1015-11 (AFNOR, 2006b).
- The apparent porosity, capillary absorption and chloride diffusion were evaluated according to French Recommendation AFPC-AFREM (AFPC 1997). All these tests were conducted on Φ 11 x H 5 cm cylindrical specimens.
- The external sulfate attack was performed on 2x2x16 cm prism specimens. The samples were immersed in sulfate solution containing 50 g/l $MgSO_4$ (5% by mass). The mass and dimensional variations were measured every 7 days. Compressive strength tests were conducted after 240 days of storage and compared to the 7-day compressive strengths of sound samples.
- The acid attack was performed on 4x4x4 cm cubic specimens immersed in a solution of H_2SO_4 (5%) and NH_4NO_3 (480 g/l). The corresponding mass variations were measured every 7 days.
- The alkali-silica reaction (ASR) tests were conducted on 2x2x16 cm prism specimens. The accelerated condition of ASR at 60°C and 100% RH was applied in accordance with the work of Idir *et al.* (2010), and expansion measurements were recorded after the containers and prisms had been cooled for 24 h at 20°C. This test was based on Standard NF P 18-454 (NF 2004) and designed for concrete, although it has since been validated on mortars (Moisson, 2005) and specimens sized 2x2x16 cm (Multon *et al.*, 2008; Idir *et al.*, 2010). The variations in mass and dimensions were measured every 7 days. Compressive strength tests were conducted after 240 days of storage and results were compared to the 7-day compressive strengths of sound samples.
- The accelerated carbonation test was carried out on 4x4x16 cm prism specimens according to French Recommendation AFPC-AFREM (AFPC 1997). The samples were preserved in a carbonation chamber at RH 65±5%, 50% CO_2 and room temperature. The carbonation effect was measured with the conventional phenolphthalein indicator and evaluated by measuring the compressive strength of specimens exposed in a carbonation chamber for 60 days and then under normal conditions up to 180 days (for a total of 240 days).

3. Results

In order to optimize the formulation of AAGC mortars, a parametric study was carried out. The parameters involved included the concentration of KOH activator solution and curing time. The mechanical properties of activated glass mortars were evaluated for the purpose of identifying the optimal condition. Under the condition subsequently chosen, the AAGC mortars were cast and tested for durability.

3.1 Optimization of the formulations

3.1.1 Choice of KOH concentration

Six KOH solution concentrations (1, 2, 3, 5, 7 and 10 mol/l) were studied. The compressive strength and flexural strength were measured after 7 days of curing at 60°C (Fig. 3 a, b). Fig 3 a shows that the compressive strength is not proportional to KOH concentration, since an optimal concentration was obtained at 3 mol/l. When the concentration exceeded 3 mol/l, the compressive strength decreased. This phenomenon was observed for all three recycled glasses. Fig. 3b indicates similar results for flexural strength, which reached a maximum value at 3 mol/l for G_F and G_H glasses. For the G_W glass, a fluctuation was observed between the concentrations of 3 mol/l and 7 mol/l.

[Insert Fig. 3 here]

Fig. 3: Effect of KOH concentration on the (a) compressive strength and (b) flexural strength of the AAGC mortars - curing at 60°C (RH ~ 100%) for 7 days

The alkaline solution plays two roles in geopolymer synthesis. First, alkali metal cations alter the geopolymer structural formation by virtue of their charge-balancing role (Duxson *et al.*, 2007). In addition, OH^- ions, acting as a catalyst, attack the Si-O and Al-O bonds, leading to an initial dissolution of the aluminosilicate species. The dissolved Si and Al species regroup with the geopolymer network, while at the same time releasing OH^- ions (Davidovits, 2002). Khale and Chaudhary (2007) summarized the effect of alkali concentration on mechanical properties. These authors considered that a high alkali concentration favors the formation of aluminosilicate as the dominant geopolymer product, which is also beneficial to the formation of C-S-H gel, thus resulting in increased mechanical strength with the presence of a calcium source in the mixture. However, a higher alkali concentration does not systematically lead to improved mechanical properties. The alkali concentration mainly influences the pH of the geopolymer mixture. A higher pH environment makes the geopolymer specimen more fluid and less viscous by favoring the dissolution of aluminosilicate sources, although it is less favorable for geopolymer network formation (Phair and Van Deventer, 2001; Provis and Van Deventer, 2007). The suitable pH value for geopolymer formation lies around 13~14 (Khale and Chaudhary, 2007; Phair and Van Deventer, 2002). An appropriate alkaline solution concentration is thus necessary for the development of mechanical properties. In this work, the optimal KOH solution concentration was found at roughly 3M. The optimal effect had already been highlighted by other authors. For example, Wang *et al.* (2005) showed that metakaolin-based geopolymers had a higher compressive strength at 10 M NaOH concentration. The optimum for fly ash was determined to be 12M for Palomoa *et al.*(1999) and 14 M of NaOH for Phair and Van Deventer (2002). These solutions are corrosive and handling must be done with caution.

Cyr *et al.* (2012) worked on glass powder-based geopolymers and found that the best mechanical properties were obtained for a 5M NaOH or KOH concentration; however, they did not study the 3M concentration level. This

optimal effect might be explained by the fact that at low concentrations (< 3 mol/l), the siliceous network in the glass is not sufficiently attacked by the alkaline solution and therefore fewer reaction products are formed (Cyr *et al.* (2012)). When concentrations exceed 3M, the glass bead are probably attacked so fast that products might form around the glass grains and the reaction would enter a diffusional system. The attack on glass grains would be slowed and impeded by this layer (Cyr *et al.* (2012)).

In general, for materials commonly used in geopolymer synthesis, it appears that high concentrations are required to obtain good mechanical properties, though such is not the case for glass. This finding could be explained by the high alkali content (≈13% Na_2Oeq). An alkaline activation, while minor at first, is still necessary to attack the siliceous network of the glass. This attack causes a release of alkalis from the glass, with these alkalis then being available in the reaction medium to activate the sound glass network, which would make this reaction a chain reaction.

3.1.2 Choice of curing time

With the chosen KOH concentration of 3 mol/l, the specimens were tested for compressive strength at 7 or 14 days, following different curing times at 60°C and RH ~100%. For the 7-day tests, the mortars were cured at 60°C for 1, 2, 4 and 7 days, with the remainder of curing at room temperature (20°C). The 14-day strength tests were conducted on samples stored at 60°C at all times. Fig. 4 shows the compressive strength at 7 and 14 days, as a function of the particular curing regime.

[Insert Fig. 4 here]

Fig.4 : Effect of curing time on the 7-day or 14-day compressive strength of specimens prepared with 3 mol/l KOH solution activating the glasses and then cured at 60°C (RH ~ 100%)

Effect of type of glass:

The curing time exerted an impact on all glasses, yet G_H was more heavily impacted than the other two (G_F, G_W). For short curing times, G_F and G_W glasses show similar evolution, while G_H displays lower values at early ages (1, 2 and 4 days) but at 7 days still reaches the same compressive strength as G_F and G_W. No plausible explanations stemming from the chemical composition or physical properties could be found; the reasons for such a result might be related to the glass structure, which in turn could modify the dissolution kinetics. Further investigations with NMR should be carried out in order to fully understand this result.

Effect of curing time:

It is observed that curing time has a significant effect on specimen compressive strength, independent of the nature of the glass: the longer the curing time, the greater the compressive strength. Extending the curing time from 1 to 7 days at 60°C increased compressive strength by a factor of 5. The linear trend of this increase in compressive strength suggests that it would be possible to obtain better results with longer curing. This was the reason why thermal treatment was prolonged to 14 days at 60°C. However, only a slight rise in compressive strength was observed between days 7 and 14, corresponding to rates of 1, 1 and 0 MPa/day for G_F, G_H and G_W glasses, respectively. Consequently, it would not seem necessary to extend thermal treatment beyond 7 days. Thus, the durability tests were started and conducted on samples stored for 7 days at 60 °C and 24h at 20 °C.

Depending on the intended application for this material, acceptable strength values could even be reached at one day, as shown by the G_F sample, which was close to 10 MPa after 24 h of curing at 60°C.

In the literature, geopolymer binder based on metakaolin is known to have a rapid hardening, normally just 1 day to achieve 80% of its maximum compressive strength at high curing temperature (Komnitsas and Zaharaki, 2007; Khale and Chaudhary, 2007). Blast furnace slags tend to have short setting times unlike fly ashes which have longer setting time (Nath and Sarker, 2014). In some cases, the addition of cement shortens the setting and hardening times, mainly for fly ashes. For the specimens in this work, 7 days were needed to achieve a satisfactory compressive strength, so this behavior is similar to that of fly ash.

This phenomenon can be attributed to the more highly polymerized structure of soda-lime glass compared to precursors such as slag or metakaolin, since soda-lime glass is mainly composed of Q3 and Q4 species silica (Jones *et al.*, 2001). Moreover, it might also be related to the low aluminum content and absence of alkali-silicate solutions to activate these glasses. The availability of aluminum in the reactive geopolymer mixture determines both the kinetics of gel formation and compressive strength development (Fernandez-Jimenez and Palomo in Provis, 2007). In their works, Mohammadinia *et al.,* (2019) discussed various factors that may affect the compressive strength of alkali-activated materials and their difference to geopolymers. Calcium content and Si / Al ratios of precursors are important and determining factors. Calcium-rich systems facilitate the hydration and formation of CASH gels called alkali-activated materials, and low-calcium systems and silica- and alumina-rich precursors facilitate the formation of aluminosilicate gels called geopolymers. For the latter, the best mechanical strengths are obtained for a ratio of Si /Al = 2. Although the kinetics of gel formation appear to be longer than with metakaolin or slag-based geopolymer, they still yield a satisfactory compressive strength after 7 days of curing, i.e. approx. 50 MPa.

3.2 Durability of glass powder mortars

The durability test specimens were prepared with 3 mol/l KOH and cured at 60°C for 7 days. Prior to testing, the samples were cooled at room temperature for 24 h. Carbonation, chloride penetration and sulfate attack are the three critical durability factors due to their adverse effect in aggressive environments; also, these factors are correlated with the water absorption and permeability of materials (Bernal *et al.*, 2014; Hossain *et al.*, 2015).

3.2.1 Transfer properties

The durability of concrete mainly depends on the transport of aggressive substances (like Cl^- and SO_4^{2-}) in the concrete matrix. As indicators of concrete durability, apparent porosity, capillary absorption and diffusion provide information on pores and the transport status of the concrete. Apparent porosity gives the percentage of open pores to the total apparent volume of the concrete. Capillary absorption is the measure of a material's ability to spontaneously absorb and transmit water by means of capillary suction. The diffusion coefficient reflects the kinetics of ion penetration into the concrete matrix.

Table 2 shows the results of the studied specimens. Cement mortar is presented here for purposes of comparison with the specimens. Let's note that the transfer properties of AAGC are stronger than those of Portland cement mortar.

The porosity of all three alkali-activated glasses was higher than that of cement mortar, which means that these alkali- activated specimens are less dense and more porous. During the alkali- activation reaction, all water does not participate in the formation of products but serves as the main support of reactions (Xu and Van Deventer, 2000; Rees *et al.*, 2008; Duxon *et al.*, 2007; Van Deventer *et al.*, 2007). This released water causes pores to form.

This process can explain the high porosity of g alkali- activated mortars compared to cement mortars. Figure 5 enables visualizing the apparent porosity of mortars. In comparing the 3 glasses, it is noted that glass G_W is the least porous.

[Insert Fig. 5 here]

Fig. 5: State of the specimens after exposure to chemical attack

The diffusion coefficient values show a threefold difference with respect to mortar cement. This finding can be explained by the ability of the cement matrix to better attach chloride ions. Consequently, the ions spread to a lesser extent.

Considering the dispersion of results, alkali- activated specimens have a capillary coefficient some 5 times greater than that of cement mortar. This outcome corroborates the results of the other two properties studied herein, i.e. porosity and diffusion coefficient. These conclusions are in perfect agreement with Albitar *et al.* (2017), who compared geopolymers made from fly ash to cement pastes.

Table 2: Transfer properties of the alkali- activated samples synthesized by a 3 mol/l KOH solution activating the glass, cured at 60°C for 7 days (RH ~ 100%)

[Insert Table 2 here]

As previously reported by Zhang *et al.* (2017), controversy exists surrounding the performance of Alkali-Activated Materials (AAM) vs. Portland cement concretes in terms of water absorption and permeability. Some authors (Shi, 1996; Rodríguez *et al.*, 2008; Mithun and Narasimhan, 2016) have shown that the water permeability of AAM is less than that of OPC, while others support the opposite (Bernal *et al.*, 2010; Yang *et al.*, 2016), although in both cases their works were conducted on alkali-activated slag. The results of this study align with the first group. A number of authors (Borges *et al.*, 2016) have related transfer properties to the silica content of the materials: capillary absorption increases with the silicate content category of alkali-activated materials. For Zhang *et al.* (2017), transfer properties depend on a set of factors, namely: the modulus of activators, water/binder ratio, precursor type, curing time, activator concentration, SiO_2/Al_2O_3, and drying duration, which in turn governs gel chemistry and pore structure.

3.2.2 Resistance to sulfates

Sulfate attack was carried out on the specimens through immersion in a 5% $MgSO_4$ solution. The dimensional and mass variations were measured for up to 218 days (Fig. 6). Mass expansion and increase was detected in the initial measurements (at 2 days) on all three specimens, which can be attributed to water intake into the pores. After that, no distinct variation in dimensions or mass was observed until the last measurement. A white precipitation was observed on the sample surface and in the solution as of the first week of conservation in sulfate solution. This phenomenon had already been reported in the literature (Sigh *et al.*, 2013). According to Albitar *et al.* (2017), this white precipitate is composed of sodium carbonate (Na_2CO_3), which originates from the reaction between the leached sodium hydroxide of the specimens and atmospheric carbon dioxide (CO_2). G_H specimens showed less precipitation than the other two specimens. In this study, the glass was activated with KOH, which implies that the reaction products would, in this case, be potassium carbonate (K_2CO_3). At the end of the test, no visual degradation (surface erosion, cracking) was observed for all three specimens.

OPC deterioration is generally attributed to the formation of expansive products within a concrete exposed to sulfate sources. Ettringite is considered to be the main deteriorated product and is formed by the reaction of sulfate ions with aluminate hydrate (Tylor, 1997). Cements, which have limited aluminum content, were however also subjected to deterioration by sulfate attack (Idiart, 2011). Controversy thus arose over whether the formation of gypsum through the reaction of calcium hydroxide (CH) and sulfate ions leads to expansion (Tian and Cohen, 2000). In this work, the low aluminum content in specimens considerably decreases the possibility of ettringite formation during exposure to sulfate solution. The calcium content (8~12%) in the raw materials can cause gypsum formation, which might explain the observation of white precipitation. No expansion or degradation was observed however for these specimens until the end of the test (218 days), which demonstrates that the specimens were not susceptible to sulfate attack.

According to the literature, AAM tend to exhibit excellent sulfate resistance for various kinds of precursors: fly ash (Fernandez-Jimenez *et al.*, 2006; Djwantoro *et al.*, 2014; Albitar *et al.*, 2017), clay (Slaty *et al.*, 2015), palm oil fuel ash (Yusuf, 2015), and slag (Wang *et al.*, 2016). Zhang *et al.* (2017) compiled the work completed on geopolymer behavior withstanding sulfate attack. According to their conclusions therefore, the resistance of geopolymers to a type of sulfate depends on the calcium content of the precursors: high-calcium alkali-activated materials are less resistant to Na_2SO_4, as opposed to a low-calcium alkali-activation level, which would be more resistant to $MgSO_4$. This finding is due, according to Bakherv (2005), to the migration of alkaline ions into the contact solution. Compared with Portland cement, AAGC exhibit better sulfate behavior, which according to Sata *et al.* (2012) is owed to the reaction products (alkali-activation reaction products), being more stable than C-S-H (cement hydration products).

[Insert Fig. 6 here]

Fig. 6: Variations in (a) dimensions and (b) mass vs. time for the specimens immersed in $MgSO_4$ solution

3.2.3 Resistance to carbonation

In this study, the method used has been phenolphthalein spraying, which allows characterizing the carbonation front of the material. Phenolphthalein was sprayed on the section perpendicular to the surface exposed to carbonation; this section was obtained after cutting out the specimen. As shown in Fig. 7 for all three types of glass, no front (visual sign) of carbonation appears and the entire specimen surface became shaded pink, which appeared at a pH greater than 9.5 (AFPC-AFREM 97). This result could indicate that if indeed carbonation was present, it did not cause a drop in pH below 9.5. The high solubility of sodium carbonate potentially formed might also be cited as a cause, given that species can easily diffuse inside the porous network.

In an ordinary cement-based concrete, the carbon dioxide contained in the air may react with the hydrated cement. When carbon dioxide diffuses inside the concrete, in the presence of water, it first reacts with portlandite (hydrated lime, $Ca(OH)_2$) to form calcium carbonate (calcite, $CaCO_3$). This formation leads to a decrease in the concrete pore solution pH, which in turn causes the depassivation of steels, i.e. a pH below 11.4 (Parrot, 1987).

Carbonation in alkali-activated glass is different than in Portland-based systems, since no portlandite is being formed. Moreover, the glass alkali (13% by weight) dissolve and maintain a high pH value. However, the carbonation of alkali compounds can occur, hence other types of carbonates can be formed in this type of product. Idir *et al.* (2011) observed the presence of sodium carbonates in glass precipitates attacked by an NaOH solution. Bernal *et al.* (2012) and Pouhet and Cyr (2016) both observed the formation of alkali carbonate

compounds in alkali-activated slag and alkali-activated metakaolin, respectively. The stabilization pH of these types of carbonates was greater than 10.6 and therefore not low enough to be revealed by phenolphthalein; this outcome would ascribe significant chemical stability to steels.

The mechanism implemented to carry out the carbonation reaction for Portland cements is very well known, and standardized tests exist to define its kinetics. Few studies however treat this mechanism for the case of alkali-activated materials (Bernal *et al.*, 2012; Pouhet and Cyr, 2016) and the corresponding standardized tests are not yet in place.

As with the transfer properties, the carbonation process of AAM is influenced by both precursors and activators. In order to improve the resistance to carbonation in the cases of slag, metakaolin and fly ash, some authors (Badar *et al.*, 2014) suggested the use of a high activator concentration or else reduction of the precursor Ca content. Using Na_2SiO_3 instead of sodium carbonates would reduce carbonation (Deja, 2002). The curing conditions (natural environment or accelerated tests) also exert an effect on the carbonation of AAM. Bernal *et al.* (2012) found that as CO_2 concentration increased, sodium bicarbonate appeared, accompanied by a monohydrate sodium carbonate and calcite (Bernal *et al.*, 2014). While in the natural environment, calcite is the major carbonation product of AAM (Bernal *et al.*, 2013). The accelerated carbonation, under which this study's specimens are kept (RH of 65±5% and 50% CO_2), promotes the formation of large amounts of sodium bicarbonate. To obtain more reliable and representative results, Zhang *et al.* (2017) recommended an accelerated carbonation of AAM at a CO_2 concentration of less than 1% and an RH of 65 ± 5%.

As regards the efflorescence risks of AAM widely reported in the literature (Škvára *et al.*, 2009; Pacheco-Torgal *et al.*, 2010; Kani *et al.*, 2012; Pouhet and Cyr, 2016), these do not appear to occur for AAGC under the present test conditions. Upon completion of the accelerated carbonation tests, no efflorescence is present on the specimen surface. This result can be explained by the low concentration of activating solutions used in the study compared with those used for metakaolin or slag-based geopolymers (Kani *et al.*, 2012; Cihangir *et al.*, 2015), as well as by the high curing temperature, which would reduce the appearance of efflorescence (as demonstrated by Zhang *et al.* (2014) for the case of fly ash). The combination of high temperature and low concentration of active solution serves to accelerate the geopolymerization reaction while reducing the availability of moving alkalis (and activating solution), which would have crystallized on the surface and caused this efflorescence.

[Insert Fig. 7 here]

Fig. 7: Sections of specimens preserved under accelerated carbonation conditions, with a demonstration using phenolphthalein of the sound and non-carbonated (colored) condition

3.2.4 Resistance to acid

Fig. 8 presents the mass variations of specimens G_F, G_H and G_W immersed in: (a) 5% H_2SO_4 solution (pH=0.5), and (b) 480 g/l of NH_4NO_3 solution (pH=4.7) up until 220 days. The fluctuations at the initial measurements, until 16 days, were caused by water intake into the specimen pores. Regardless of the solution, all three specimen types experienced a similar trend of mass loss: rapid mass reduction followed by stabilization of the curves. For the H_2SO_4 solution, the stabilized values were -1.07%, -0.88% and -1.39% for G_F, G_H and G_W, respectively. At the end of the test, the solutions were still acidic with a pH value around 2.2 (ΔpH = 1.7). For the NH_4NO_3 solution, the mass loss was greater, with the stabilized values being -1.45%, -0.71% and -1.46% for

357 G_F, G_H and G_W, respectively. The final pH value was approx. 8.4, meaning that more alkali was being leached
358 (ΔpH = 3.7). In comparing these three specimen types, it can be noted that G_W had a much higher mass loss
359 while G_H produced the lowest values of mass variation regardless of the acid. This result may be in contradiction
360 with porosity, whose G_w sample value is lower than either G_H or G_F. One explanation lies in the type of pores:
361 smaller, more numerous, more interconnected and more tortuous in the case of G_w (Zajac *et al.*, 2018), which
362 would facilitate leaching.
363 Alkali-activated materials are considered to have better resistance to acid attack than OPC (Fernandez-Jimenez
364 *et al.*, 2007; Albitar *et al.*, 2017), a finding possibly attributed to the stable AAM network and its low (or even
365 absence of) calcium, as well as to its high alkalinity, capable of neutralizing H^+ ions and altering the aggressive
366 environment. Degradation however has still been observed in extreme acidic environments. Davidovits *et al.*
367 (1999) found a 7% mass loss for a metakaolin-based geopolymer immersed in 5% H_2SO_4 solution for 4 weeks.
368 Under the same acid attack condition, Bakharev (2005) studied a fly ash-based geopolymer with different
369 activators and found mass losses between 2% and 12%. Song *et al.* (2005) studied a fly ash-based geopolymer in
370 10% sulfuric acid and obtained a mass loss below 3% within 4 weeks. Allahverdi and Škvára (2001, 2005)
371 summarized the degradation mechanism as the de-alumination of the Al-O-Si structure and formation of an
372 imperfect siliceous structure due to framework vacancies. In this work, the alkali- activation products seemed to
373 be stable in the acidic solution, as the mass loss obtained was less than 2%. This slight mass loss can be
374 attributed to the leaching of excessive alkaline ions in the solution, which consequentially increased the solution
375 pH value. Degradation signs were observed, although they were less significant than those detected in OPC
376 under the same conditions. As shown in Fig. 9, the specimens immersed in sulfuric acid were cracked, and the
377 G_H-based specimens appeared to better resist than those made from G_F and G_W. The specimens preserved in
378 nitric acid did not sustain any degradation regardless of the type of glass used.
379 [Insert Fig. 8 here]

380 Fig. 8: Mass variation for specimens immersed in (a) 5% H_2SO_4 solution, and (b) 480 g/l of NH_4NO_3 solution

381 ***3.2.5 Resistance to the alkali-silica reaction***
382 Fig. 9 provides the dimensional and mass variations of specimens preserved at 60°C, RH ~ 100% for accelerated
383 alkali-silica reaction testing. The first-week expansion (~0.4%) could be due to water intake into the pore
384 structure. Let's note however that compared to samples held in sulfate solution, the initial water intake was 0.1%,
385 and the remaining 0.3% might be related to rapid swelling due to the alkali-silica reaction, as is often the case for
386 opal in accelerated tests (Moisson, 2005). After the first week, the dimension was found to have varied by only a
387 small amount during the 220 days of measurements, regardless of the type of recycled glass. Similar
388 observations could be made for the mass, as specimens gained 1-2% mass after the first week. Beyond that time,
389 the mass was found to decrease slightly, to within 1%. This mass loss with time was most likely caused by
390 leaching of excessive alkali in the specimens.
391 ASR is considered to be the "cancer" of OPC concrete; it generally involves the attack of reactive silica by alkali
392 to form N,K-C-S-H gel in the presence of calcium. This gel can expand by absorbing the water and ultimately
393 cause concrete damage. Opal and some glass aggregates are known to be harmful components in concrete due to
394 their high contents of glassy SiO_2, which is highly reactive in forming ASR gel (Moisson, 2005; Gao, 2010). The
395 same concern thus arose regarding the use of recycled glass in this work since the high reactive silica content
396 levels are vulnerable to attack in the alkaline environment and can form ASR gel in the presence of calcium. No

expansion however was observed and these results are in accordance with the literature. The rare works conducted on the alkali-silica reaction in alkali-activated systems have revealed that negligible or no expansion was observed despite the high alkali content. According to Li *et al.* (2006): "*A geopolymer does not generate any dangerous alkali-silica reaction because there are not enough free alkalis to react with the aggregates in order to create alkali-silica gel.*" Na^+ and K^+ are fixed in the cavities of the SiO^{-4} and AlO^{-4}, thus counterbalancing the negative charge of Al^{3+}.

This phenomenon can only explain a portion of our observations. The reactive silica in the recycled glass forms N (K)-S-A-H products and ASR gel in an alkaline environment because of the low aluminum content in the glass. Another part of the explanation would thus lie in the grain size used in this study (30 µm). Idir *et al.* (2010) showed that gels stemming from the reaction of glass powder with an average grain size below 950 µm are not highly expansive. SEM analysis has indicated that two kinds of products could be found: N (K)-S-A-H (C in Fig. 10), and ASR gel (B in Fig. 10). This result confirms that AAGC have a good resistance to RAS. The gels formed by the glass reaction in a basic environment are not or only slightly expansive.

The behavior of alkali-activated materials in withstanding the alkali-silica reaction remains relatively good in spite of the strong presence of alkali in the medium. In cement-based materials, the alkali-silica reaction is closely correlated with the alkali content of the mixture. Two reactions can indeed take place. The first, i.e. the alkali-silicate reaction (ASR), which results from the reaction of aggregates with a reactive silica and the alkali present in the mixture. This reaction produces a gel that swells in the presence of moisture and causes expansion and damage to the concrete. The second reaction, i.e. alkali-carbonate reaction (ACR), results from the reaction of aggregates with dolomite and alkali present in the mixture. The latter reaction is less common than the ASR. Compared to OPC, alkali-activated materials display a different behavior in the presence of the alkali-silica reaction (Al-Otaibi, 2008). For these authors, alkali-activated concrete has a low susceptibility to ASR expansion due to alkali binding in the hydration products. For other authors, as reported by Leemann *et al.*, the low calcium content of the precursor lies at the origin of this effect, given the important role of calcium in the ASR process (Leemann *et al.*, 2011). When the sensitivity of AAM to the alkali-silica reaction has been demonstrated, high-calcium materials are to be used, like in the case of blast-furnace slag (Bakharev *et al.*, 2001; Chen *et al.*, 2012).

[Insert Fig. 9 here]

Fig. 9 : Variations in (a) dimension and (b) mass vs. time for specimens preserved at 60°C and 100% RH

[Insert Fig. 10 here]

Fig. 10 : SEM micrograph and EDX of glass particle for G_F(A), amorphous alkali-silicate gel (B) and reaction products (C) - mortar cured at 60°C and 100% RH for 240 days

4. Discussion

The results presented in this work prove that a consolidated material can be obtained by activating recycled glass with an alkaline solution (KOH) under certain curing conditions (activator concentration, temperature, time, etc.). An appropriate concentration of KOH solution (3 mol/l), an extended curing time (7 days) and a high temperature (60°C) are all necessary to achieve acceptable mechanical performance. As one of the advantages compared to metakaolin-based geopolymers, the synthesis of AAGC does not require the addition of water glass (Cyr *et al.*, 2012).

The durability tests demonstrated that AAGC mortars synthesized from recycled glass show good resistance to sulfate attack, carbonation and the alkali-silica reaction. These materials displayed only a small loss of soluble parts during an acid attack. The evaluations however were conducted on the measurements of dimensional and mass variations. To complete the necessary information, the evolution of compressive strength before and after durability testing was also studied (as shown in Fig. 11). The variation in compressive strength was calculated as the difference between strength after 240 days of testing and that after initial curing.

It can be seen that the variation in compressive strength depends on the type of tests (conservation environment) as well as on the type of recycled glass. For tests like sulfate attack (A), alkali-silica reaction (C), curing at 20°C without exchange (E) (i.e. conservation in plastic bags and no exchange with the external medium), all three types of specimens display little variation in compressive strength. For the remainder of the test, these AAGC presented different losses in mechanical performance. The reason for degradation can be tied to the dissolution of soluble parts in the solution. When specimens were immersed in the solution, the soluble parts did dissolve. This dissolution might involve both the leaching of alkali into the conservation solution and the de-alumination of the alkali-activated materials structure. The leaching of alkali in water has been confirmed in the literature (Cyr *et al.*, 2012), and this may be the primary reason for degradation in a solution medium. All three specimen types show different degrees of mechanical loss: 50.4% and 21.3% for G_F, 29.6% and 15% for G_H, and 61.5% and 27.8% for G_W after the sulfuric acid and ammonium nitrate attacks, respectively. The de-alumination phenomenon was reported by Allahverdi and Škvára (2001, 2005) as the degradation mechanism in acid attack rupturing the Al-O-Si bond and forming an imperfect siliceous structure due to framework vacancies. Compared with the NH_4NO_3 solution, H_2SO_4 generated much more degradation for the specimens: 50% for G_F, 30% for G_H, and 62% for G_W. These recycled glasses have the relatively low contents of aluminum; the high dissolution in the solution can be attributed to a lack of aluminum for stabilizing alkali in the alkali-activated materials structure, which is in agreement with the literature (Cyr *et al.*, 2012).

G_H, however, stands out from the other two glasses (G_F and G_W) by its good behavior in the presence of most media, except for acid attacks. To compare the resistance to durability test among the three specimen types, the ratio of the surface area (shown in color) to the surface area of the range -100% ~0 is calculated by taking the integral of the surface. These ratios equal 59.6% for G_F, 80.7% for G_H and 42.1% for G_W, respectively. G_H showed the best resistance to durability during testing. This finding could be attributed to its high Al/Si ratio (0.034) compared with that of G_F (0.012). The low Al/Si value could be correlated with the lower hydraulic stability and high fraction of alkali released during leaching tests. Although G_W has an Al/Si ratio (0.033) similar to that of G_H, its greater particle size may be the main reason behind its poor durability resistance.

[Insert Fig. 11 here]

Fig. 11: Comparison of compressive strength before and after treatment in different environments - a positive value indicates a higher compressive strength after treatment

The preceding paragraphs have provided a brief summary of information derived on the sustainability behavior of alkali-activated materials (AAM). These findings are however to be treated cautiously since they result from standardized tests on concrete, mortars or pastes transposed to AAM. At present, no standardized tests specific to this type of material are available. Teams, notably from RILEM (Provis and Winnefeld, 2013), are setting up specific tests for such material. Their initial recommendations will soon be published.

From a global perspective, AAGC exhibit the same sustainability behavior as alkali-activated materials made with other precursors (metakaolin, fly ash, blast-furnace slag), except for carbonation, with glass behaving much better.

5. Conclusion

This study has confirmed the possibility of synthesizing alkali-activated materials based on different sources of recycled glass. The following conclusions can be drawn:

- The compressive strength depends on the concentration of the activating solution as well as on curing time at a temperature of 60°C.
- The optimal concentration of activating solution (KOH) is 3 mol / l, regardless of the type of glass;
- Between 1 and 7 days, the longer the curing time at 60°C, the better mechanical performance from the mortar;
- Increasing curing time to 14 days does not yield any significant gain in compressive strength, and in some cases a slight drop can even be recorded (G_W);

The paper has also presented an experimental campaign to study the durability of the materials obtained, as assessed by durability indicators (porosity accessible to water, capillarity and chloride ion diffusion coefficients), and behavior of the material in sulfate and acidic solutions as well as in high CO_2 concentrations and with respect to the alkali-silica reaction condition.

The conclusions are:

- The AAGC studied are more permeable than Portland cement-based mortars;
- The transfer properties of AAGC typically vary depending on the type of glass used: porosity is lower for the G_W-based AAGC and equivalent for the other two glasses. Lower absorption and diffusion coefficients for the chloride ions are recorded for the G_H-based AAGC
- The AAGC studied herein exhibit good resistance to acid and sulfate attacks as well as to the alkali-silica reaction. All three types of AAGC studied exhibit nearly the same behavior;
- Compressive strength is affected differently depending on the conservation environment. Acid attacks cause the most significant decline in terms of mechanical strength. Although the specimens displayed apparent defects (cracks), it appears that the attack with ammonium nitrate weakened the specimens, resulting in lower compressive strength. Conservation without exchange and under alkali-reaction test conditions (i.e. 60°C) leads to an increase in compressive strength.

6. References

AFNOR. (2006a), NF EN 196-1 Méthodes d'essais des ciments - Partie 1 : Détermination des résistances mécaniques, avril.

AFNOR. (2006b), NF EN 1015-11 Méthodes d'essai des mortiers pour maçonnerie - Partie 11 : détermination de la résistance à la flexion et à la compression du mortier durci.

AFNOR. NF EN 196-6 April 2012, Methods of testing cement - Part 6: determination of fineness

AFNOR. NF P18-454. (2004) Béton – Réactivité d'une formule de béton vis-à-vis de l'alcali réaction– Essai de performance ; December.

AFPC-AFREM. (1997). Méthodes recommandées pour la mesure des grandeurs associées à la durabilité, Compte-rendu des journées techniques AFPC-AFREM « Durabilité des bétons », Toulouse, 1997.

Albitar M., Mohamed Ali M.S., Visintin P., Drechsler M. (2017). Durability evaluation of geopolymer and conventional concretes, Construction and Building Materials 136, 374–385.

Allahverdi A., skvara F., (2001), Nitric acid attack on hardned paste of geopolymeric cements', ceremaics-slikaty, 45(4), 143-149

Allahverdi A., skvara F., (2005), sulfuric acid attack on hardned paste of geopolymeric cements', ceremaics-slikaty, 49, 225

Al-Otaibi S (2008), Durability of concrete incorporating GGBS activated by water-glass, Construction and Building Materials 22 (2008) 2059–2067.

Aly Z., Vance E.R., Perera D.S., Hanna J.V., Griffith C.S. and Davis J. Durce D. (2008). Aqueous leachability of metakaolin-based geopolymers with molar ratios of Si/Al = 1.5-4, Journal of Nuclear Materials 378:172-179

Badar S M., Kupwade-Patil K., Bernal S.A., Provis J.L., Allouche E.N. (2014). Corrosion of steel bars induced by accelerated carbonation in low and high calcium fly ash geopolymer concretes, Construction and Building Materials. 61 79–89.

Bakharev T. (2005). Durability of geopolymer materials in sodium and magnesium sulfate solutions, Cement and Concrete Research. 35 (6) 1233–1246.

Bakharev T. (2005). Resistance of geopolymer materials to acid attack, Cement and Concrete Research 35, 658–670.

Bakharev T. Sanjayan J.G. and Cheng Y.B. (2001). Resistance of alkali-activated slag concrete to alkali-aggregate reaction. Cement and Concrete Research, 31 (2): 331-334.

Bernal S., De Gutierrez R., Delvasto S., Rodriguez E. (2010). Performance of an alkali activated slag concrete reinforced with steel fibers, Construction and Building Materials, 24 (2) 208–214.

Bernal S.A., Provis J.L., Brice D.G., Kilcullen A., Duxson P., van Deventer J.S.J. (2012) Accelerated carbonation testing of alkali-activated binders significantly underestimates service life: the role of pore solution chemistry, Cement and Concrete Research. 42 (10) 1317–1326.

Bernal S.A., Provis J.L., Green D.J. (2014). Durability of alkali-activated materials: progress and perspectives, Journal of the American Ceramic Society, 97 (4) 997–1008.

Bernal S.A., Provis J.L., Walkley B., San Nicolas R., Gehman J.D., Brice D.G., Kilcullen A.R., Duxson P., van Deventer J.S.J. (2013). Gel nanostructure in alkali-activated binders based on slag and fly ash, and effects of accelerated carbonation, Cement and Concrete Research. 53 127–144.

Bernal S.A., San Nicolas R., Myers R.J., Mejía de Gutiérrez R., Puertas F., van Deventer J.S.J., Provis J.L. (2014). MgO content of slag controls phase evolution and structural changes induced by accelerated carbonation in alkali-activated binders, Cement and Concrete Research. 57 33–43.

Borges P.H.R., Banthia N., Alcamand H.A., Vasconcelos W.L., Nunes E.H.M., (2016). Performance of blended metakaolin/blastfurnace slag alkali-activated mortars, Cement and Concrete Composites. 71 42–52.

Chen J H., Huang J S., Chang Y W., (2011). Use of reservoir sludge as a partial replacement of metakaolin in the production of geopolymers, Cement and Concrete Composites, 33 (5), 602-610.

552 Cihangir F., Ercikdi B., Kesimal A., Deveci H., Erdemir F (2015). Paste backfill of high-sulphide mill tailings
553 using alkali-activated blast furnace slag: Effect of activator nature, concentration and slag properties.
554 Minerals Engineering, 83,117–127
555 Cyr M. Idir R. and Poinot T. (2012). Properties of inorganic polymer (geopolymer) mortars made of glass cullet,
556 Journal of Materials Science, 47:2782–2797.
557 Davidovits J, (2002). 30 Years of Successes and Failures in Geopolymer Applications. Market Trends and
558 Potential Breakthroughs.Geopolymer, Conference, October 28-29, Melbourne, Australia.
559 Davidovits J. (1991). Geopolymers: inorganic polymeric new materials, Journal of Thermal Analysis, 37:1633-
560 1656.
561 Davidovits J. (1993). Geopolymer cement to minimise carbon-dioxide greenhouse warming, Ceramic
562 Transactions, 37:165-182.
563 Davidovits J. Buzzi L. Rocher P. Gimeno D. Marini C. et Tocco S. (1999). Geopolymeric cement based low cost
564 géopolymer materiels results from the European project Geocostem, geopolymer proceeding, 83-96.
565 Deja J. (2002). Carbonation aspects of alkali activated slag mortars and concretes, Silicates Industriels, 67 (1)
566 37–42.
567 Djwantoro S.E.W., Hardjito, D Sumajouw M.J., Vijaya Rangan B. (2004). On the development of fly Ash-based
568 geopolymer concrete, ACI materials journal. 101 (6) 467–472.
569 Duxson P. Fernandez-Jimenez A. Provis J.L. Lukey G.C. Palomo A. et Van Deventer J.S.J. (2007). Geopolymer
570 technology: the current state of the art, Journal of Materials Science, 42:2917-2933.
571 Fernandez-Jimenez A., García-Lodeiro I., Palomo A. (2007). Durability of alkali activated fly ash cementitious
572 materials, Journal of Materials Science. 42 (9) 3055–3065.
573 Gao, XX (2010). Contribution to the requalification of alkali silica reaction (ASR) damaged structures:
574 assessment of the ASR advancement in aggregates by alkali silica reaction, phd thesis, INSA, Toulouse.
575 Hajimohammadi A., van Deventer J.S.J. (2017). Solid reactant-based geopolymers from rice hull ash and sodium
576 aluminate, Waste and Biomass Valorization, 8 (6) 2131-2140.
577 Hossain M.M., M.R. Karim, M.K. Hossain, M.N. Islam, M.F.M. Zain. (2015). Durability of mortar and concrete
578 containing alkali-activated binder with pozzolans: a review, Construction and Building Materials. 93 95–109.
579 Idiart, A. E., López, C. M., & Carol, I. (2011). Chemo-mechanical analysis of concrete cracking and degradation
580 due to external sulfate attack: A meso-scale model. Cement and Concrete Composites, 33(3), 411–423.
581 Idir R., Cyr M, Tagnit-Hamou A. (2010). Use of fine glass as ASR inhibitor in glass aggregate mortars,
582 Construction and Building Materials, 24 (7) 1309-1312.
583 Idir R., Cyr M, Tagnit-Hamou A. (2011). Pozzolanic properties of fine and coarse color-mixed glass cullet,
584 Cement and Concrete Composites, 33 (1) 19-29.
585 Jones A.R, Winter R, Greaves G.N, Smith I.H (2001). MAS NMR study of soda-lime–silicate glasses with
586 variable degree of polymerisation, Journal of Non-Crystalline Solids, 293–295, 87-92.
587 Kabir S., Alengaram U.J. (2015). Jumaat M.Z, Sharmin A., Islam A., Influence of Molarity and chemical
588 composition on the development of compressiv strength in POFA based geopolymer mortar, Advances in
589 Materials Science and Engineering. 2015 1–15.
590 Kani E.N., Allahverdi A., Provis J.L. (2012). Efflorescence control in geopolymer binders based on natural
591 pozzolan, Cement and Concrete Composites. 34 (1) 25–33.

592 Ke X., Bernal S.A., Ye N., Provis J.L., Yang J. (2015). One-part geopolymers based on thermally treated red
593 Mud/NaOH blends, Journal of the American Ceramic Society. 98 5–11.
594 Khale D., Chaudhary R., (2007). Mechanism of geopolymerization and factors influencing its development: a
595 review, Journal of Materials Science, 42, 729–746
596 Komljenović M. Baščarević Z. et Bradić V. (2010). Mechanical and microstructural properties of alkali-activated
597 fly ash geopolymers, Journal of Hazardous materials, 181:35-42.
598 Komnitsas K, Zaharaki D, (2007). Geopolymerisation: a review and prospects for the minerals industry, Miner.
599 Eng. 20: 1261–1277.
600 Leemann A., Le Saout G., Winnefeld F., Rentsch D., Lothenbach B. (2011). Alkali–Silica Reaction: The
601 Influence of Calcium on Silica Dissolution and the Formation of Reaction Products, journal of the American
602 ceramic society, 94, 1243-1249.
603 Li K L, Huang G H, Chen J. (2006). Cai Y B, Jiang L H, Study on Abilities of Mineral Admixtures and
604 Geopolymer to Restrain ASR. Engineering Materials 302-303:248-254.
605 Maragkos I. Giannopoulou I.P. et Panias D. (2009). Synthesis of ferronickel slag-based geopolymers, Minerals
606 Engineering, 22:196-203.
607 Mithun B.M., Narasimhan M.C. (2016). Performance of alkali activated slag concrete mixes incorporating
608 copper slag as fine aggregate, Journal of Cleaner Production. 112 837–844.
609 Mohammadinia A, Arulrajah. A, Sanjayan. J, Disfani. M. M, Win Bo. M, Darmawan S. (2016), Stabilization of
610 demolition materials for pavement base/subbase applications using fly ash and slag geopolymers: Laboratory
611 investigation, Journal of Materials in Civil Engineering, 28: 7
612 Moisson M. (2005). Contribution à la maîtrise de la réaction alcali-silice par ajout de fines de granulats réactifs
613 dans le béton, Thèse de doctorat INSA, Toulouse.
614 Mozgawa W. and Deja J. (2009). Spectroscopic studies of alkaline activated slag geopolymers, Journal of
615 Molecular Structure, 926:434-441.
616 Multon S, Cyr M, Sellier A, Leklou N, Petit L. (2008). Coupled effects of aggregate size and alkali content on
617 ASR expansion. Cement and Concrete Research, 38(3):350–9.
618 Nath P, Sarker P.K. (2014), Effect of GGBFS on setting, workability and early strength properties of fly ash
619 geopolymer concrete cured in ambient condition. Construction and Building Materials, 66:163-171
620 Nath P, Sarker P.K. (2015), Use of OPC to improve setting and early strength properties of low calcium fly ash
621 geopolymer concrete cured at room temperature. Cement and Concrete Composites, 55, pp.205-214
622 Pacheco-Torgal F., Jalali S. (2010). Influence of sodium carbonate addition on the thermal reactivity of tungsten
623 mine waste mud based binders, Construction and Building Materials. 24 (1) 56–60.
624 Palomo A, Grutzeck M. W, Blanco M.T. (1999), Alkali-activated fly ashes: a cement for the future, Cement and
625 Concrete Research, 29: 1323-1329
626 Panias D. Giannopoulou I.P. and Perraki T. (2007). Effect of synthesis parameters on the mechanical properties
627 of fly ash-based geopolymers, Physicochemical and Engineering Aspects, 301:246-254.
628 Parrot Jean. (1987). A review of carbonation in reinforced concrete, Cement and Concrete Association, 1987, p.
629 42.

Peng M.X., Wang Z.H., Shen S.H., Xiao Q.G., Li L.J., Tang Y.C., Hu L.L. (2017). Alkali fusion of bentonite to synthesize one-part geopolymeric cements cured at elevated temperature by comparison with two-part ones, Construction and Building Materials. 130, 103-112.

Phair J.W., Van Deventer J.S.J. (2002). Effect of the silicate activator pH on the microstructural characteristics of waste-based geopolymers, International Journal of Mineral Processing, 66: 121-143.

Phair JW, Van Deventer JSJ (2001). Minerals Engineering 14:289. Effect of silicate activator pH on the leaching and material characteristics of waste-based inorganic polymers.

Pouhet R., Cyr M. (2016). Carbonation in the pore solution of metakaolin-based geopolymer, Cement and Concrete Research, volume 88, pages 227-235.

Provis J L. and Winnefeld F. (2013). RILEM Réunion Internationale des Laboratoires et Experts des Matériaux, Systèmes de Construction et Ouvrages, Technical Committee 247-DTA Durability testing of alkali-activated materials.

Provis, J. L, van Deventer J. S. J, (2007). Geopolymerisation kinetics. 2. Reaction kinetic modelling, Chemical Engineering Science, 62 (9), 2318-2329.

Prud'homme E.Michaud P. Joussein E. Peyratout C. Smith A. Arrii-Clacens S. Clacens J.M. et Rossignol S. (2010). Silica fume as porogent agent in geo-materials at low temperature, Journal of the European Ceramic Society, 30:1641-1648.

Rees C.A., Provis J.L., Lukey G.C., Van Deventer J.S.J. (2008). The mechanism of geopolymer gel formation investigated through seeded nucleation. Colloids and Surfaces A: Physicochemical and Engineering Aspects, vol. 318, pp. 97-105.

Rodríguez E., Bernal S., Gutiérrez R.M.d., Puertas F. (2008). Alternative concrete based on alkali-activated slag, Materiales de Construcción. 58 (291) 53–67.

Sata V., Sathonsaowaphak A., Chindaprasirt P. (2012). Resistance of lignite bottom ash geopolymer mortar to sulfate and sulfuric acid attack, Cement and Concrete Composites. 34 (5) 700–708.

Shi C. (1996). Strength pore structure and permeability of alkali activated slag mortars, Cement and Concrete Research. 26 (12) 1789–1799.

Škvára F., Kopecký L., Šmilauer V., Bittnar Z. (2009). Material and structural characterization of alkali activated low-calcium brown coal fly ash, Journal of Hazardous Material. 168 (2) 711–720.

Slaty F., Khoury H., Rahier H., Wastiels J. (2015). Durability of alkali activated cement produced from kaolinitic clay, Applied Clay Science. 104 229–237.

Stanton T.E. (1940). Expansion of concrete through reaction between cement and aggregate, Proceedings of the American Society of Civil Engineers, 66; 1781-811.

Sturm P., Gluth G.J.G., Brouwers H.J.H., Kühne H. (2016). Synthesizing one-part geopolymers from rice husk ash, Construction and Building Materials. 124 961–966.

Taylor HFW. Cement Chemistry (2nd edition). (1997) Thomas Telford: New York; 1997.

Tian B., Cohen M. D. (2000). Does gypsum formation during sulfate attack on concrete lead to expansion? Cement and Concrete Research, 30 (1), 117–123.

Van Deventer J.S.J., Provis J. L., Duxson P., Lukey G. C. (2007). Reaction mechanisms in the geopolymeric conversion of inorganic waste to useful products. Journal of Hazardous Materials A, vol. 139, pp. 506–513.

669 Wang H., Li H., Yan F. (2005). Synthesis and mechanical properties of metakaolinite-based geopolymer,
670 Colloids and Surfaces A: Physicochemical and Engineering Aspects, 268:1-6.
671 Wang W.C., Chen B.T., Wang H.Y., Chou H.C., A. (2016). Study of the engineering properties of alkali-
672 activated waste glass material AAWGM, Construction and Building Materials. 112 962–969.
673 Xu H., Van Deventer J.S.J. The geopolymerisation of alumino-silicate minerals. (2000). International Journal of
674 Mineral Processing, vol. 59, pp. 247–266.
675 Yang K., Yang C., Magee B., Nanukuttan S., Ye J. (2016). Establishment of a preconditioning regime for air
676 permeability and sorptivity of alkaliactivated slag concrete, Cement and Concrete Composites. 73 19–28.
677 Yusuf M.O. (2015). Performance of slag blended alkaline activated palm oil fuel ash mortar in sulfate
678 environments, Construction and Building Materials. 98 417–424.
679 Zajac M, Skocek J, Adu-Amankwah S, Black L, Ben Haha M. (2018). Impact of microstructure on the
680 performance of composite cements: Why higher total porosity can result in higher strength. Cement and
681 Concrete Composites, 90, 178–192
682 Zhang J, Shi C, Zhang Z, Ou Z, (2017). Durability of alkali-activated materials in aggressive environments: A
683 review on recent studies, Construction and Building Materials, 152, 598–613.
684 Zhang J., Shi C, Zhang Z, Ou Z. (2017). Durability of alkali-activated materials in aggressive environments: A
685 review on recent studies, Construction and Building Materials, 152 598–613.
686 Zhang Z, Provis J. L, Reid A and Wang H. (2014), Fly ash-based geopolymers: The relationship between
687 composition, pore, structure and efflorescence, Cement and Concrete Research, 64 30–41
688 Zibouche F, Kerdjoudj H, D'Espinose de Lacaillerie J.B et Van Damme H. (2009). Geopolymers from Algerian
689 metakaolin - Influence of secondary minerals, Applied Clay Science, 43:453-458

Investigations on the durability of alkali-activated recycled glass

Rachida IDIR[a*], Martin CYR[b], Alexandre PAVOINE[a]

[a] Cerema, DIMA Project team, 120, rue de Paris - BP 216 - Sourdun - 77487 Provins CEDEX

[b] Université de Toulouse, UPS, INSA, Laboratoire Matériaux et Durabilité des Constructions, 135, avenue de Rangueil, F-31077 TOULOUSE Cedex 4, France

*Corresponding author: Rachida IDIR

Phone: (+33) 1 60 52 34 04

Email: rachida.idir@cerema.fr

Flat glass (G_F) **Hollow glass (G_H)** **Windshield glass (G_W)**

Fig. 1: Glass powders obtained after grinding

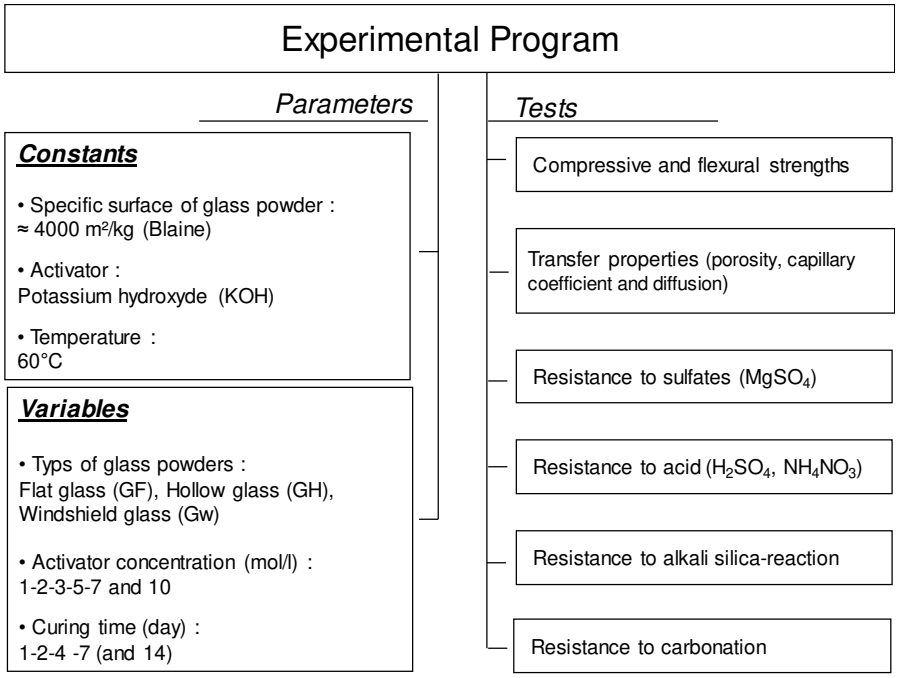

Fig. 2 : Summary of the experimental program part of the study

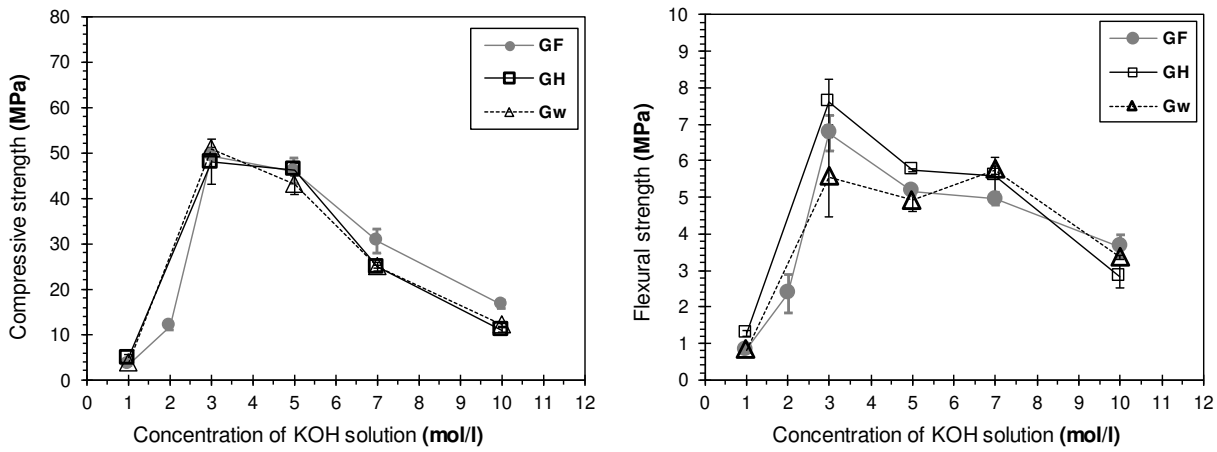

(a) (b)

Fig.3 : Effect of KOH concentration on the (a) compressive strength and (b) flexural strength of the AAGC mortars - curing at 60°C (RH ~ 100%) for 7 days

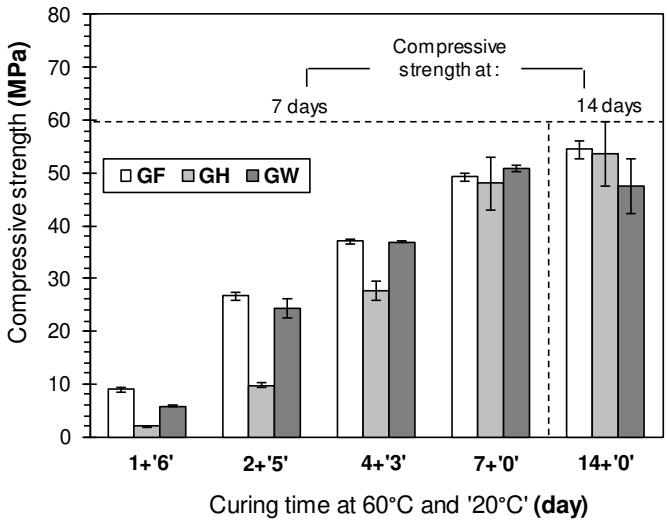

Fig.4 : Effect of curing time on the 7-day or 14-day compressive strength of specimens prepared with 3 mol/l KOH solution activating the glasses and then cured at 60°C (RH ~ 100%)

19

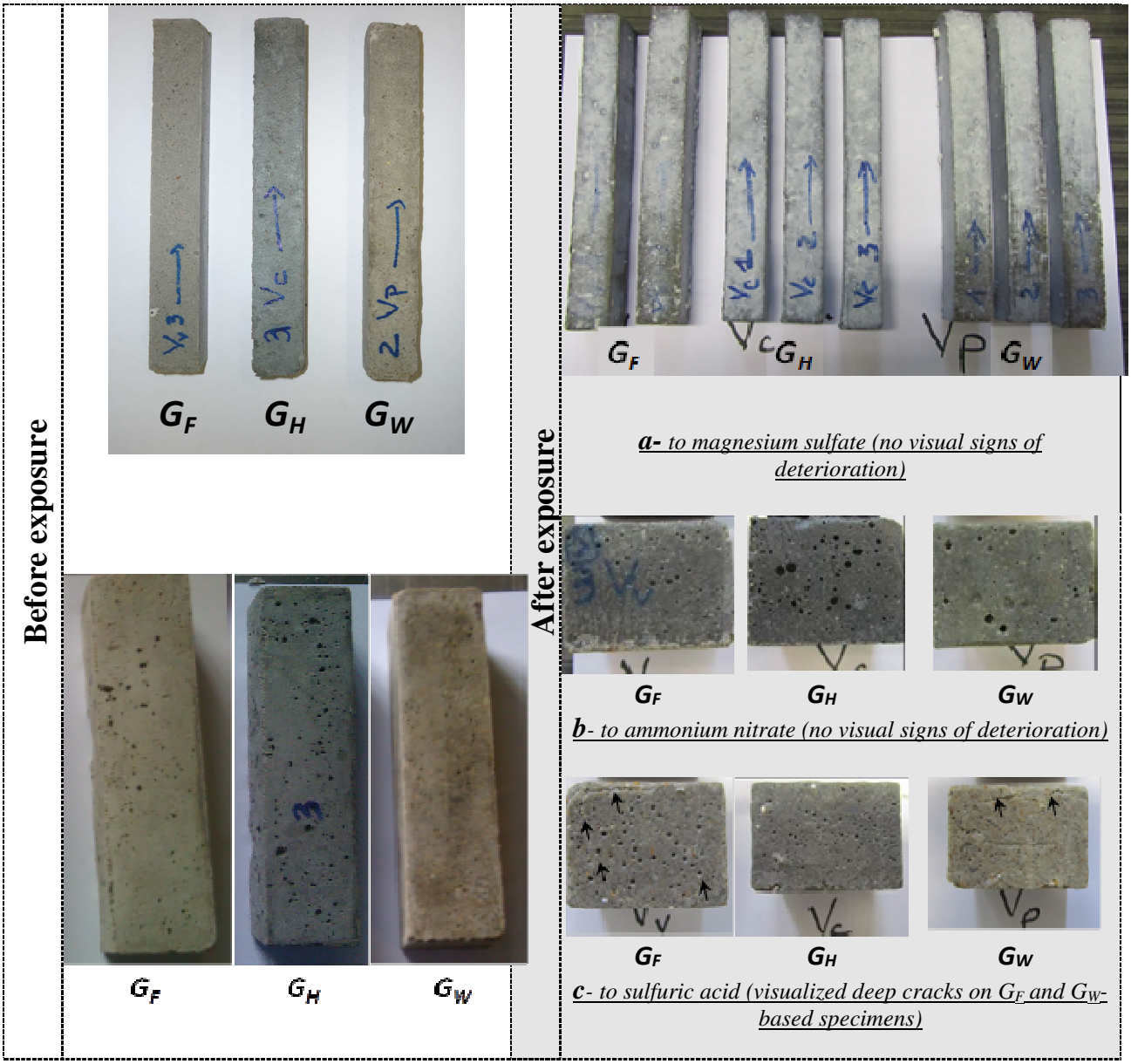

Fig.5 : State of the specimens after exposure to chemical attack

20
21

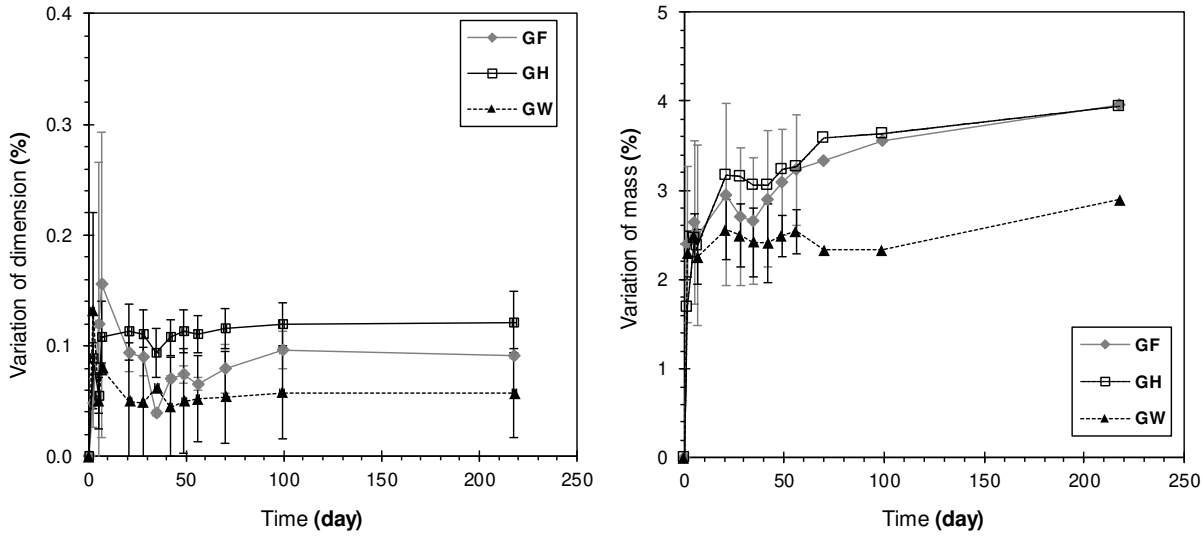

(a) (b)

Fig. 6 : Variations in (a) dimensions and (b) mass vs. time for the specimens immersed in MgSO4 solution

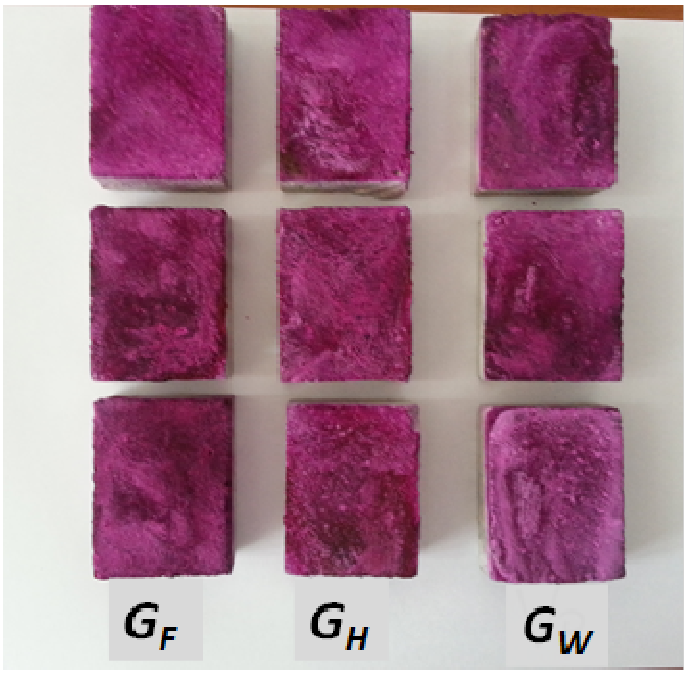

Fig. 7 : Sections of specimens preserved under accelerated carbonation conditions, with a demonstration using phenolphthalein of the sound and non-carbonated (colored) condition

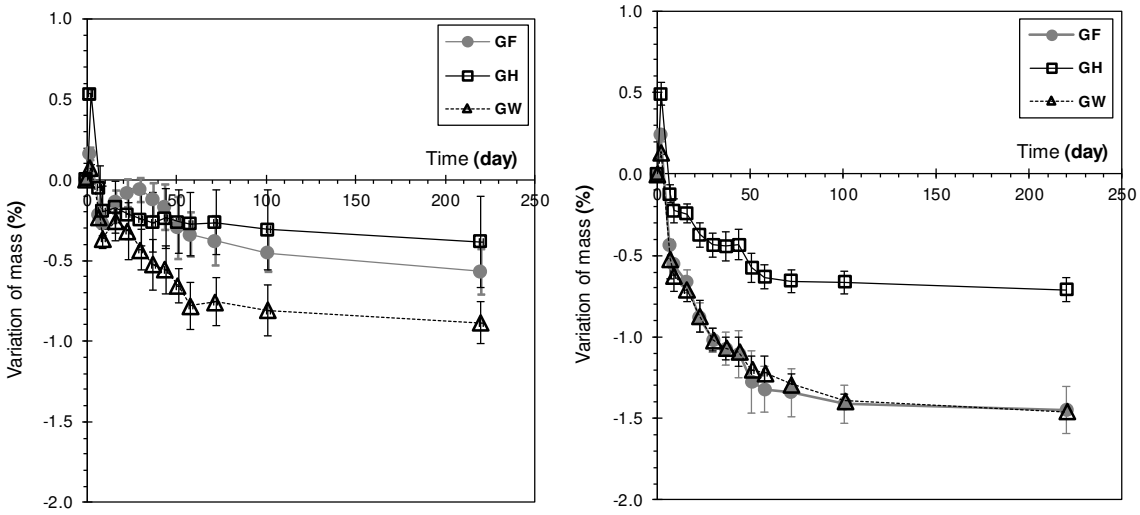

(a) (b)

Fig. 8 : Mass variation for specimens immersed in (a) 5% H_2SO_4 solution, and (b) 480 g/l of NH_4NO_3 solution

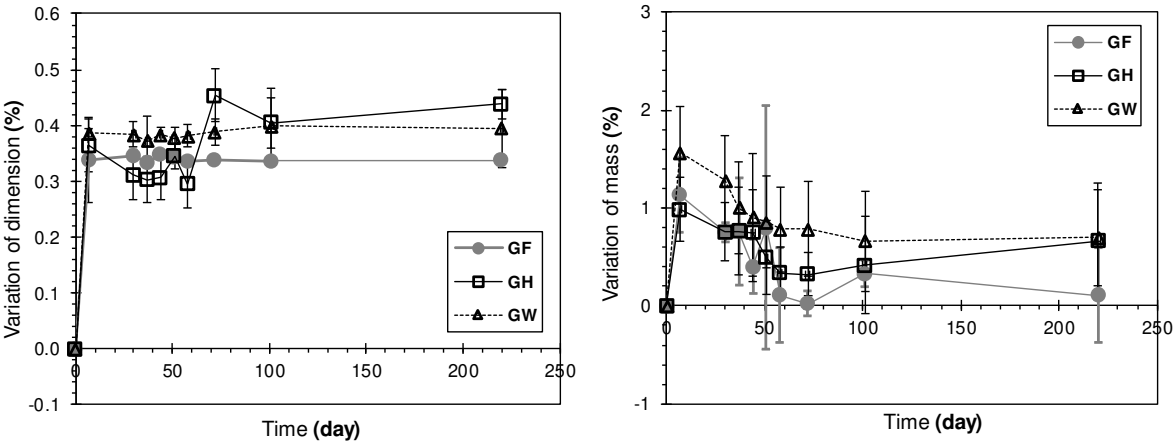

(a) (b)

Fig. 9 : Variations in (a) dimension and (b) mass vs. time for specimens preserved at 60°C and 100% RH

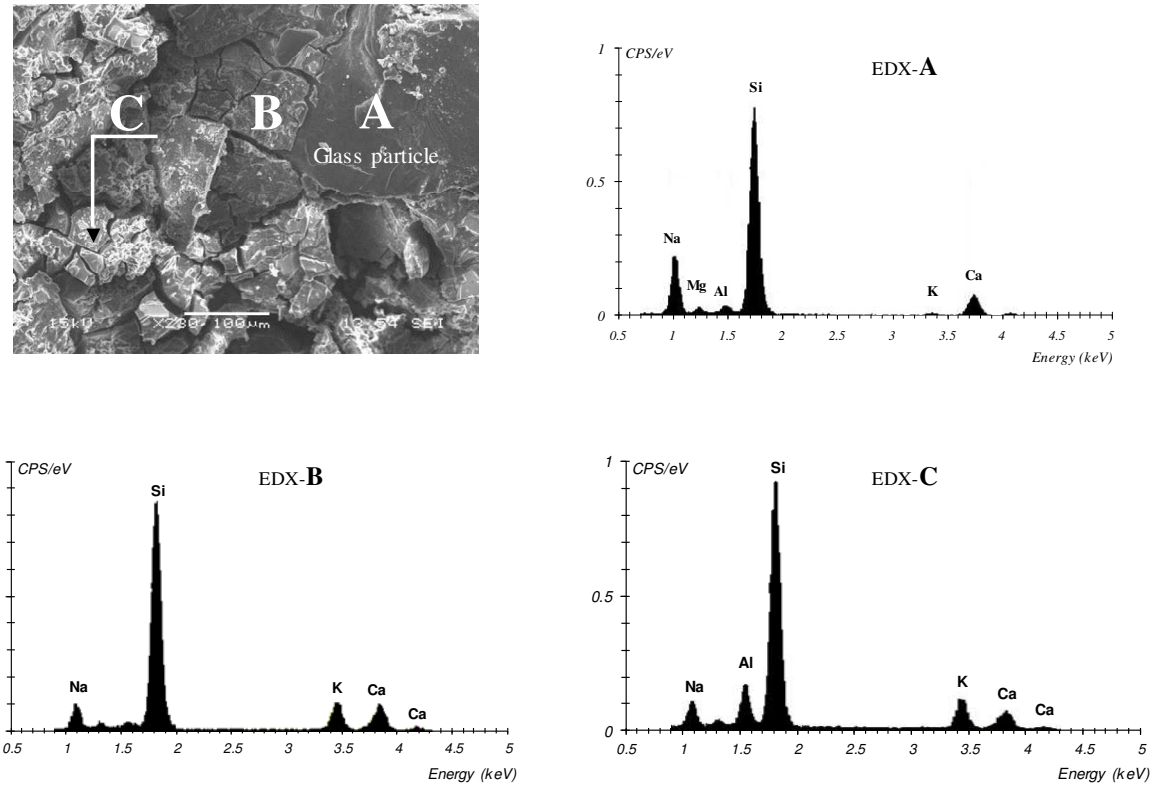

Fig. 10 : SEM micrograph and EDX of glass particle for G_F(A), amorphous alkali-silicate gel (B) and AAGC gel (C) - mortar preserved at 60°C and 100% RH for 240 days

36
37

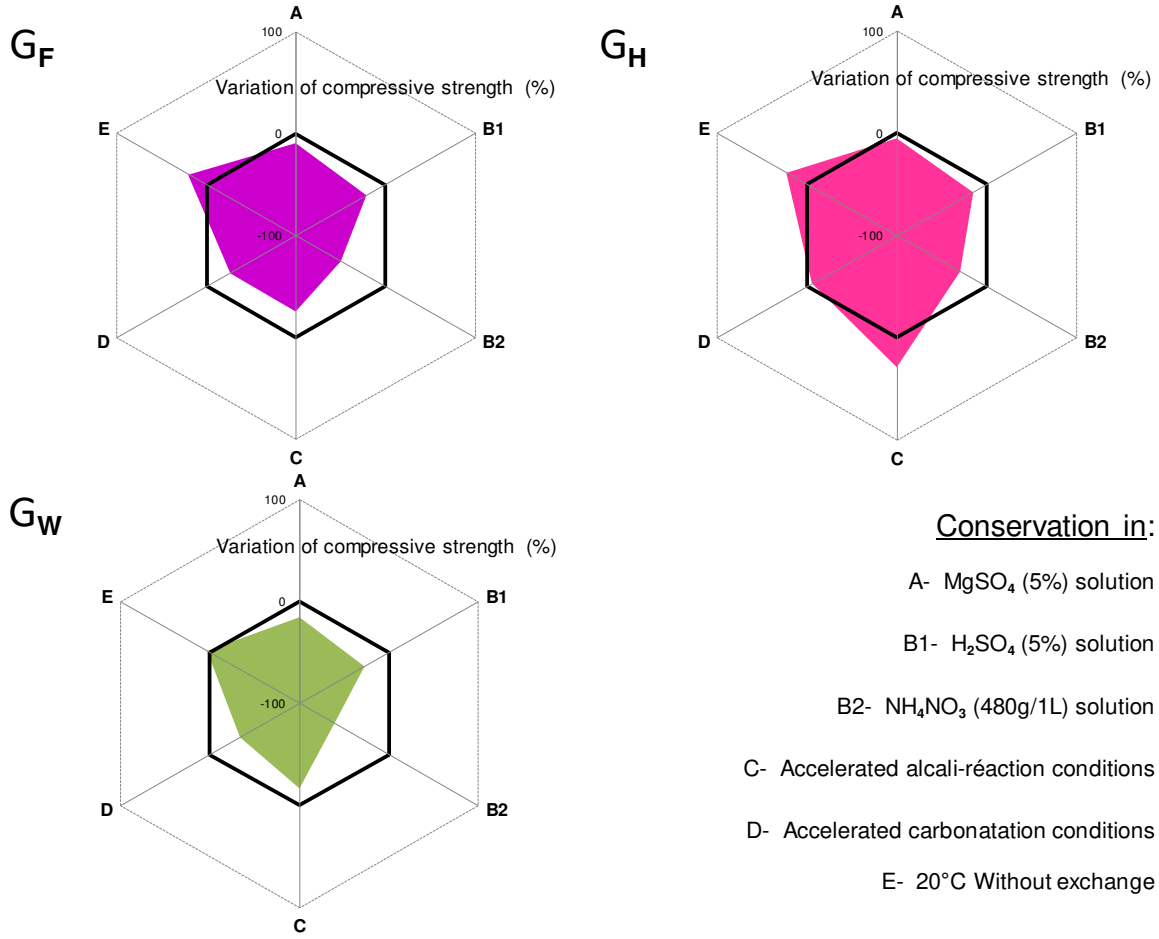

Fig. 11 : Comparison of compressive strength before and after treatment in different environments - a positive value indicates a higher compressive strength after treatment

38

Investigations on the durability of alkali-activated recycled glass

Rachida IDIR[a*], Martin CYR[b], Alexandre PAVOINE[a]

[a] Cerema, DIMA Project team, 120, rue de Paris - BP 216 - Sourdun - 77487 Provins CEDEX

[b] Université de Toulouse, UPS, INSA, Laboratoire Matériaux et Durabilité des Constructions, 135, avenue de Rangueil, F-31077 TOULOUSE Cedex 4, France

*Corresponding author: Rachida IDIR

Phone: (+33) 1 60 52 34 04

Email: rachida.idir@cerema.fr

Table 1: Physical and chemical characterizations of the studied glass types

Physical characterization								
	Flat glass (G_F)			Hollow glass (G_H)		Windshield glass (G_W)		
Specific surface area (Blaine) (cm^2/g)	3,965			4,008		4,027		
Density (cm^2/g)	2.50			2.48		2.50		
Average diameter (µm)	21.2			27.4		29.3		
Chemical composites (% mass)								
	SiO_2	Al_2O_3	Fe_2O_3	CaO	MgO	SO_3	K_2O	Na_2O
Flat glass (G_F)	72.16	0.68	0.12	7.80	4.38	0.21	0.21	14.46
Hallow glass (G_H)	69.89	1.92	1.05	12.31	1.34	0.14	0.16	13.18
Windshield glass (G_W)	70.11	1.86	1.04	11.67	1.37	0.11	0.07	13.76

Table 2: Transfer properties of the AAGC samples synthesized by a 3 mol/l KOH solution activating the glass, cured at 60°C for 7 days (RH ~ 100%)

	G_F	G_H	G_W	C Mortar*
Apparent porosity (%)	17.6±0.1	17.4±0.9	13.5±0.1	10.7
Capillary coefficient ($kg/m^2/s^{1/2}$)	0.15	0.14	0.13	0.04~0.08
Diffusion coefficient (Cl^-) ($10^{-10}m^2/s$)	2.6±0.7	1.1±0.1	1.3±0.1	~ 0.42

* Cement mortar (cement CEM I 52.5 R, Water/Cement = 0.5, age: 28 days, storage: 20°C)